Journal of Thermal Analysis, Vol. 41 (1994) 323-336

In celebration of the 60th birthday of Dr. Andrew K. Galwey

ISOTHERMAL AND RISING TEMPERATURE KINETIC STUDIES OF DOPED NONSTOICHIOMETRIC BASIC NICKEL CARBONATE

D. Fried and D. Dollimore

Department of Chemistry, The University of Toledo, Toledo, OH 43606, USA

Abstract

The techniques of thermal analysis are used to determine the mode of decomposition of nickel carbonates doped by the method of coprecipitation. Nickel carbonate prepared by this method is basic in nature with the stoichiometry $x\mathrm{NiCO_3} \cdot y\mathrm{Ni(OH)_2} \cdot z\mathrm{H_2O}$. Isothermal Thermogravimetry was applied to determine the mechanism of decomposition. Rising temperature Thermogravimetry (TG) and Differential Scanning Calorimetry (DSC) were used to study the effects of doping on the kinetics of the decomposition. Doping was found to strongly influence the kinetics of the decomposition. The kinetics of thermal decomposition of the doped carbonates were compared with conductivity studies. A compensation effect has been observed and is discussed, in the thermal decomposition of the doped nickel carbonates.

Keywords: DSC, kinetics, nickel carbonates, solid state decomposition, TG

Introduction

In previous publications, the effect of doping on cadmium carbonate [1, 2] and on manganous carbonate [3] with reference to the mode of decomposition and surface area [4] were studied. In other publications the kinetics of the thermal decomposition of various carbonates were reported [5–8]. In all these studies the emphasis was on the kinetics of decomposition, based on models to be found in two reviews [9, 10]. As noted the effect of doping is to cause variations in the kinetics of decomposition [1], the surface area [4] and the final solid residue [11] which are functions of the type of dopant and its concentration. Here we deal with the effect of doping on the kinetics of the decomposition of nickel carbonate. Surface area measurements on various residues from the thermal decomposition of nickel oxysalts, which included the carbonate, have been studied by Dollimore and Pearce [4]. In the other carbonate systems examined with

John Wiley & Sons, Limited, Chichester
Akadémiai Kiadó, Budapest

specific reference to the kinetics of decomposition, the effect of doping by coprecipitation [3], the application of rising temperature kinetics [5] and the appearance of a compensation effect were all demonstrated.

The above effects are the subject of this study on nickel carbonate. The matter is complicated by the basic nature of the nickel carbonate. The formula given for precipitated nickel carbonate varies in the literature. Stoichiometries of $NiCO_3{\cdot}NiO{\cdot}2H_2O$ [11, 12], $NiCO_3{\cdot}H_2O$ [13], $NiCO_3{\cdot}2Ni(OH)_2{\cdot}4H_2O$ and $2NiCO_3{\cdot}3Ni(OH)_2{\cdot}4H_2O$ [14] have been reported. However, in most preparations, the formula $x NiCO_3{\cdot}y Ni(OH)_2{\cdot}z H_2O$ is assigned where the coefficients x, y, and z are a function of the concentration of the reactants, the temperature of the reaction and the prehistory of the sample [4].

Experimental

The basic nickel carbonate prepared under controlled conditions of temperature and concentrations 0.375 $mol{\cdot}l^{-1}$ aqueous solutions of nickel nitrate and ammonium carbonate were mixed at 298 K. The doped samples were prepared by adding the nitrates of lithium, silver, calcium, zinc, aluminum and chromium in ratios of one half, one, five and ten atom percent to nickel nitrate and reacting with ammonium carbonate.

Thermal analysis studies were carried out using a DuPont 1090 Thermal Analysis System with a 910 DuPont Differential Scanning Calorimeter and a Stanton Redcroft 761 Thermobalance interfaced with the Omnitherm Thermal Analysis System. The decomposition were carried out in dry nitrogen with a flow rate of 20 ml/min on 1–3 mg samples. Isothermal TG curves were obtained for the decomposition of the undoped basic nickel carbonate at temperatures of 280, 290, 300, 310, 320°C. Rising temperature TG and DSC curves were recorded for each doped sample at a heating rate of 10 $deg{\cdot}min^{-1}$.

Results and discussion

Rising temperature TG and DSC curves for pure basic nickel carbonate are shown in Fig. 1. The basic nickel carbonate decomposes in two stages. The first stage consists of the loss of waters of hydration and the second stage involves the loss of H_2O and CO_2. The kinetics of the second stage of this decomposition are discussed below for all the samples.

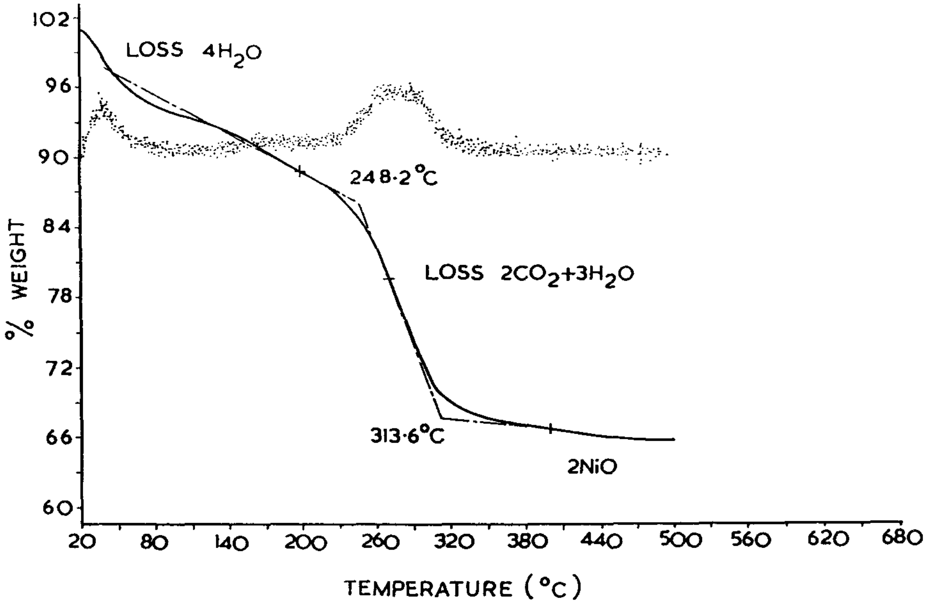

Fig 1 DSC and TG curves for basic nickel carbonate heating rate of 10 deg/min

Isothermal kinetic study on the undoped basic salt

To determine the kinetic mechanism to be applied in subsequent rising temperature experiments an isothermal study was undertaken on the undoped basic salt using the TG equipment. Each isothermal curve was converted from % mass *vs.* time to fraction decomposed (α) *vs.* the reduced time (t_r). The reduced

Table 1 Rate equations commonly used for solid state decompositions [10, 15]

Rate equation	Function of alpha $f(\alpha) = kt$
Contracting disk	$1-(1-\alpha)^{1/2}$
Contracting sphere	$1-(1-\alpha)^{1/3}$
First order	$-\ln(1-\alpha)$
Diffusion 1 Dim.	α^2
Diffusion 2 Dim.	$(1-\alpha)\ln(1-\alpha)+\alpha$
Diffusion 3 Dim.	$[1-(1-\alpha)^{1/3}]^2$
Avrami-Erofe'ev	$[-(\ln 1-\alpha)]^{1/n}$ $n=2$ *or* $n=3$
Ginstling-Brounshtein	$1-2/3\alpha-(1-\alpha)^{2/3}$

time is defined as the time divided by the time ($t_{0.5}$) required for the reaction to reach half completion. If the reaction is isokinetic, each of the α *vs.* t_r plots should be identical. The basic nickel carbonate decomposition is isokinetic up to α values of 0.6 and reduced time values of 1.2. These plots are shown in Fig. 2. A likely mechanism for the decomposition may be determined from a comparison of the α *vs.* t_r plot with a set of similar master plots of several solid state decomposition mechanisms. Mechanisms studied are listed in Table 1 [15]. The decomposition of the basic nickel carbonate salt best fitted the contracting-sphere and contracting-disk equations. In order to compare the range of applicability of these theoretical mechanisms with the experimental curves, experimental reduced time against theoretical reduced time plots are used. Theoretical reduced time values are calculated by substituting in the experimental α values into the appropriate rate equation. A straight line with a slope

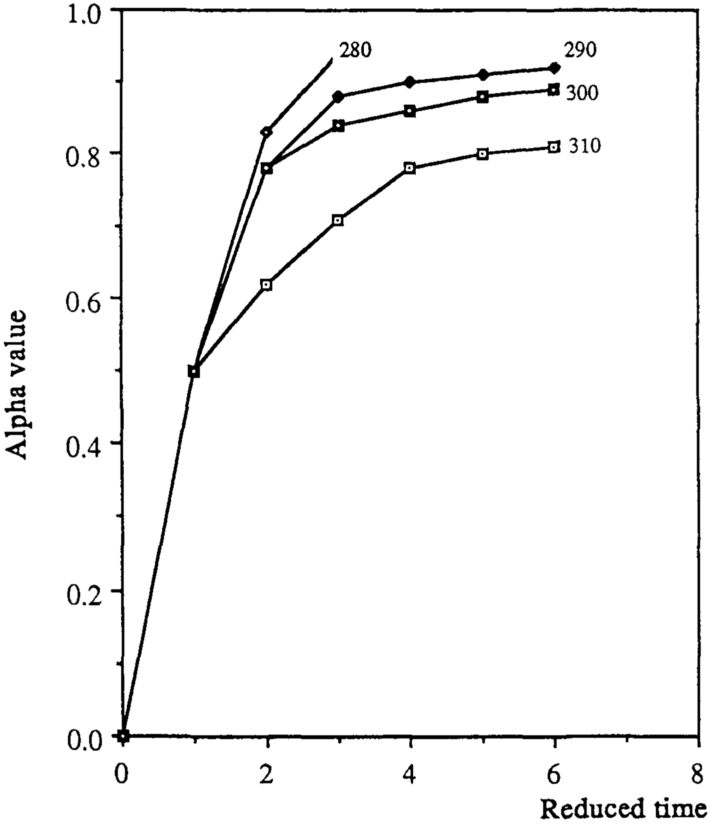

Fig. 2 Alpha reduced time plot for nickel carbonate

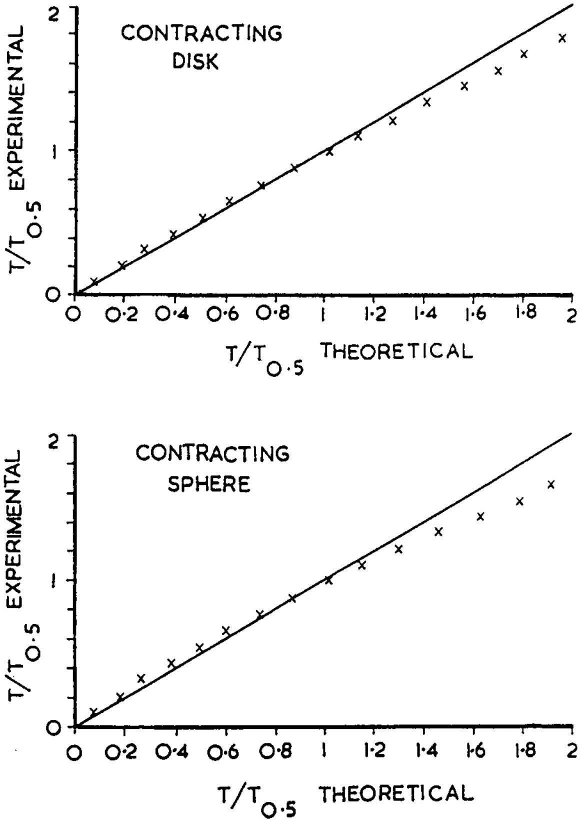

Fig. 3 Comparison on the experimental isothermal curve at 280°C with the contracting-disk and contracting-sphere rate equations

of one should result over the range of the decomposition for which that particular rate equation in applicable. Plots of the contracting-disc and contracting-sphere rate equations are shown in Fig. 3. Both fit well, but the rate constants used here were calculated from a plot of $1-(1-\alpha)^{1/2}$ *vs.* time. The rate constants were used in an Arrhenius plot. The activation energy was found to be 164 ± 4 kJ/mol with a pre-exponential factor of 1.45×10^{12} s^{-1} with an uncertainty in the value of log A of ±0.5.

Rising temperature studies

It was assumed that the rate equation in the rising temperature studies was of the same form as that found and used in the above isothermal studies on the

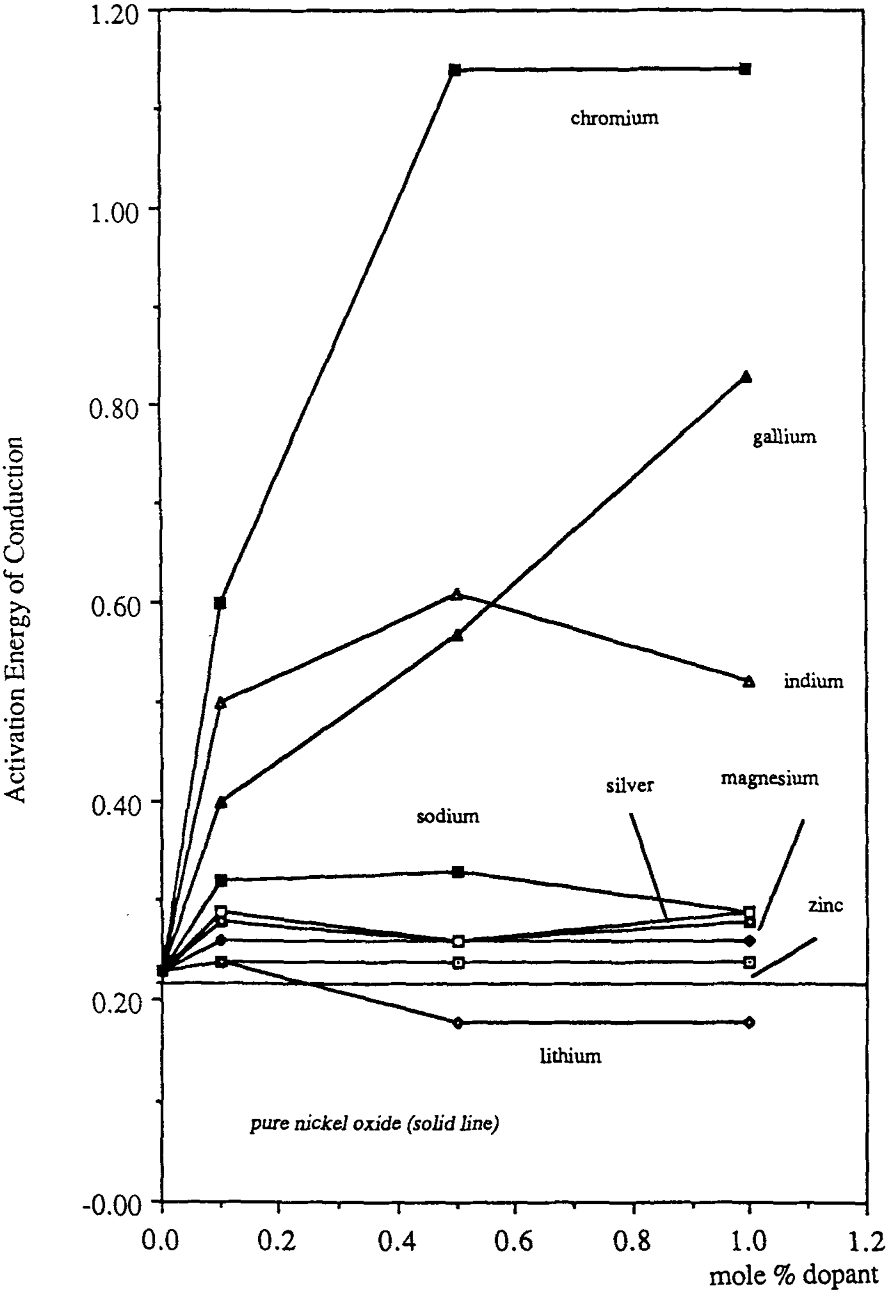

Fig. 4 Activation energy of conduction as a function of dope and in mole% [18]

undoped material. The rising temperature DSC and TG results were used to study the influence of the dopants on the activation energy and the enthalpy of the decomposition of basic nickel carbonate. The enthalpy values were calculated by integration of the DSC peaks. The activation energies, E, were determined from the rising temperature TG curves using a computer program employing the Kissinger method [16, 17] of solving the rising temperature kinetic Eq. (1).

$$\frac{\mathrm{d}\alpha}{\mathrm{d}t}=\frac{A}{b}\cdot \mathrm{e}^{-E/RT} \tag{1}$$

where b is the heating rate.

At the maximum rate of decomposition, the second derivative of the curve is equal to zero.

$$0=\frac{\mathrm{d}^2\alpha}{\mathrm{d}T^2}=\frac{AEf(\alpha)}{b\,RT^2}+\frac{\mathrm{d}(f(\alpha))}{\mathrm{d}T} \tag{2}$$

and

$$E=-\left\{\frac{\mathrm{d}(f(\alpha))}{\mathrm{d}T}\,\frac{RT^2}{f(\alpha)}\right\} \tag{3}$$

The appropriate expression of $f(\alpha)$, determined from isothermal studies, is substituted into Eq. (3).

$$f(\alpha)=(1-\alpha)^{n} \tag{4}$$

$$E=nRT^2\left(\frac{\mathrm{d}\alpha}{\mathrm{d}T}\right)_{\max}(1-\alpha)^{-1}_{\max} \tag{5}$$

By application of this technique, the kinetic parameters may be determined from only two points on the rising temperature curve. One point must be at the maximum rate of decomposition and the other point should be chosen on a suitable region of the curve in a consistent manner for each curve. The point halfway between the onset of decomposition and the rate of maximum decomposition was chosen. The values of temperature, mass loss and the first derivative for each point are substituted in Eqs (5), (6) and (7) to determine the reaction order, activation energy and the preexponential factor.

$$n=\frac{\ln\left[\dfrac{\left(\dfrac{d\alpha}{dT}\right)_1}{\left(\dfrac{d\alpha}{dT}\right)_{\max}}\right]}{\left(\dfrac{T_{\max}(T_{\max}-T_1)\left(\dfrac{d\alpha}{dT}\right)_{\max}}{T_1(1-\alpha)_{\max}}-\ln\left[\dfrac{(1-\alpha)_1}{(1-\alpha)_{\max}}\right]\right)} \tag{6}$$

$$A=b\left(\frac{d\alpha}{dT}\right)_{\max} e^{-E/RT}\,(1-\alpha)^{-n}_{\max} \tag{7}$$

The results are shown in Table 2. Significant changes in E are observed to occur with corresponding changes in the pre-exponential factors. There is a stabilization of the energy of activation values around 200–250 kJ/mol for high levels of dopant. It would seem that this is a saturation effect and that there is a limit to the incorporation of foreign ions in the lattice structure.

Schwab and Schmidt [18] have measured conductivities of doped nickel oxides. A plot of activation energies of conduction against dopant concentration is shown in Fig. 4. If this plot is compared with Fig. 5, a plot of activation energy of decomposition against dopant concentration, it can be seen that there is a decrease in the activation for conduction as the dopant level is reduced. This may signify that the nature of the large changes in activation energy from the undoped level to that found around 0.5~10% dopant level is electronic in origin. In this region the conductivity changes caused by doping may alter the rate of heat and mass transfer in the sample.

The enthalpy values shown large variations with dopant concentration. This is shown in Table 2. To explain the effect of the added dopants, enthalpy values were estimated from heat of formation data, based on the assumptions that there were no significant changes in the electronic nature of the nickel carbonate, and that the enthalpy of the decomposition is equal to the mole fraction multiplied by the enthalpy of the decomposition of each dopant metal carbonate and hydroxide. Figure 6 is a comparison of experimental enthalpy values and the values calculated as described above for the lithium and silver dopants. As can be seen in this plot, the calculated values fail to explain these large variations in enthalpy.

Figure 7 is a plot of ln A *vs.* E for the doped nickel carbonate samples. This relationship is described by the following equation:

$$\ln A = aE + b \quad a,b \text{ are constants} \tag{8}$$

and is commonly known as the compensation effect or the 'Theta Rule'. Schwab and Schmidt [18] in their study of the conductivity of the doped oxides,

Table 2 Enthalpy of decomposition and Arrhenius parameters for doped nickel carbonate

Dopant	%	Decomposition enthalpy / kJ·mol^{-1}	Activation energy / kJ·mol^{-1}	Preexponential factor / s^{-1}
Li	0.5	164	131	$1.62\cdot10^{11}$
	1.0	130	554	$3.71\cdot10^{49}$
	5.0	81.1	118	$1.85\cdot10^{10}$
	10.0	120	209	$6.21\cdot10^{15}$
Ag	0.5	178	365	$9.27\cdot10^{31}$
	1.0	93.0	304	$9.39\cdot10^{26}$
	5.0	80.5	411	$2.58\cdot10^{36}$
	10.0	84.2	209	$5.54\cdot10^{18}$
Ca	0.5	103	409	$2.24\cdot10^{36}$
	1.0	82.3	116	$1.52\cdot10^{10}$
	5.0	139	140	$3.60\cdot10^{12}$
	10.0	116	237	$4.17\cdot10^{21}$
Zn	0.5	107	340	$10.4\cdot10^{30}$
	1.0	131	407	$1.01\cdot10^{36}$
	5.0	128	243	$6.44\cdot10^{21}$
	10.0	234	209	$8.62\cdot10^{39}$
Al	0.5	114	473	$8.17\cdot10^{41}$
	1.0	79.8	205	$2.87\cdot10^{18}$
	5.0	141	168	$1.54\cdot10^{15}$
	10.0	174	256	$4.11\cdot10^{23}$
Cr	0.5	174	256	$4.11\cdot10^{23}$
	1.0	221	232	$4.08\cdot10^{21}$
	5.0	138	129	$6.10\cdot10^{11}$
	10.0	50.5	222	$2.83\cdot10^{19}$

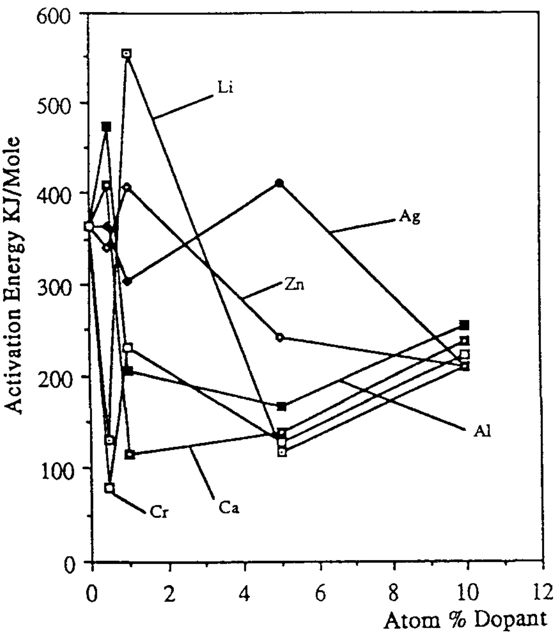

Fig. 5 Activation energy of kinetics of decomposition for doped samples

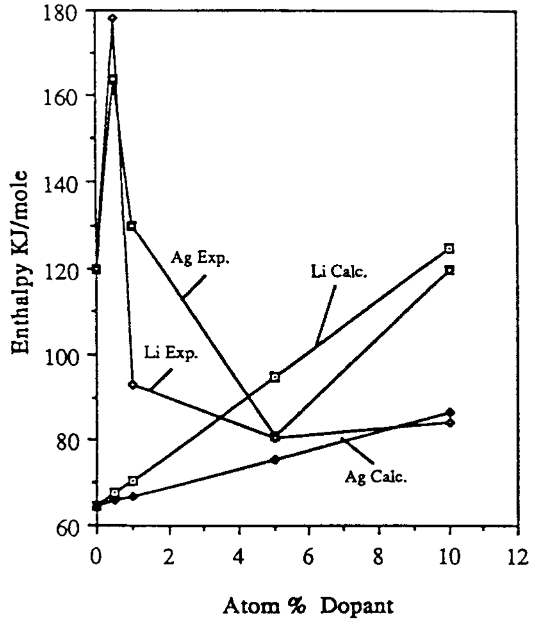

Fig. 6 Comparison of experimental enthalpy values with calculated values

found a compensation effect for the conductivity and the activation energy of conductance. Their relationship is:

$$\log \sigma_o = c + dE \tag{9}$$

where σ is the conductivity, c and d are constants, and E is the activation energy of conductance. A plot of the compensation effect observed by Schwab and Schmidt [18] for the doped nickel oxides is shown in Fig. 8.

The diverse pairs of A and E obtained for the various doped samples show a good compensation plot. The similarity between the conductivity studies of Schwab and Schmidt on the effect of the added oxides on the para-conducting nickel oxide and the kinetic results obtained here, allow one to speculate that the nonstoichiometric semiconductance of these samples is associated with the kinetics of the decomposition, and that the rate controlling step is electronic in origin. A similar step has been proposed for the decomposition of nickel oxalate [19].

$$Ni^{2+} + 2e^- \rightarrow Ni^o \tag{10}$$

In the decomposition of nickel oxalate the nickel metal can be isolated in an inert atmosphere. Here the nickel can react with the carbonate radical.

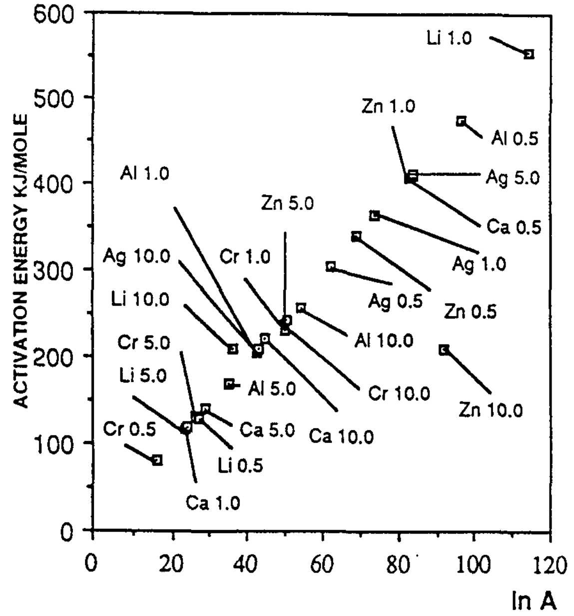

Fig. 7 Compensation effect of doped nickel carbonates

$$Ni + CO_3^{2-} \rightarrow NiO + CO_2 + 2e^- \qquad (11)$$

And the overall reaction is:

$$NiCO_3 \rightarrow NiO + CO_2 \qquad (12)$$

This is a simplistic picture for the nickel carbonates, since they actually exist in the basic form, a mixture of nickel carbonate and hydroxide, but we can use this picture to suggest that the rate-determining step is electronic in origin.

The compensation plot can be explained on the basis of several different reactions, each associated with specific values of A and E, occurring simultaneously. These values can be identified with specific kinds of locations for the reacting ionic species. These could be edge ions situated in a particular environment in the crystal structure and defects introduced by the controlled doping. Identifying each of these environments by a subscript number, to make the approach general, we have i sites. Site i is associated with values E_i and A_i and has a % population given by N_i. For the i possible sites the rum of N_i equal to 100%.

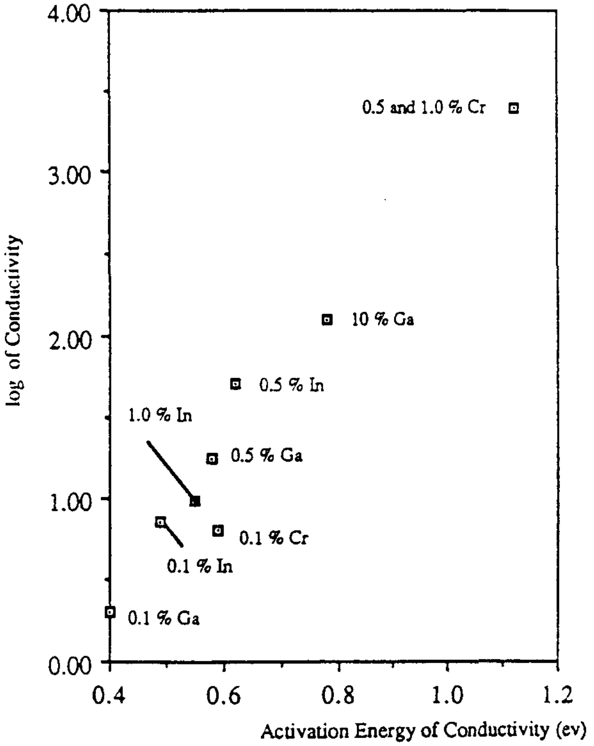

Fig. 8 Compensation effect observed by Schwab and Schmidt

The overall values of E and A for the sample are the means of the values. In a related sample, the populations are altered giving new mean values of E and A. If this model is expanded to account for a, b, c, d..., samples, then a compensation plot results from the experimental values of A and E. The matter is discussed in various publications [20–22].

The collision theory of the Polanyi-Wigner model implicitly assumes that there is a constant concentration of the precursors of product formation. However, the number of precursors per unit area and the mobilities of surface-held participants in an interface may vary with temperature. The results discussed above would support such a contention, if the rate-determining step was based on conduction. If the effective concentration of such participants is $[M]$ (possibly a composite term), the rate of product formation $[\partial P/\partial T]$ per unit area of reaction interface is:

$$\frac{\partial P}{\partial T} = A^1[M]\,e^{-E^1/RT} \tag{13}$$

where A^1 and E^1 refer to the decomposition reaction at the reaction interface, by which the reactants M are converted into products. If $[M]$ is constant within the temperature interval being studied, then the measured values of A and E refer to this process. If, however, the effective magnitude of $[M]$ varies with temperature, or from sample to sample, then a variation in the apparent Arrhenius parameters is observed. This could arise in a solid phase reaction because of variations in the total population of reacting species, or, in more complex reactions, through a sequence of consecutive steps. A model of this type is probably the cause of the effects noted in this study leading to the demonstration of a compensation effect.

A result, which helps establish the validity of the compensation effect, is stated by some authorities to be the establishment of an isokinetic temperature for a series of related reactions [23, 24]. In this study an isokinetic point exists at 315°C. This is near the general temperature of decomposition. In the doped samples the maximum rate of decomposition is in the range of 270 to 320°C.

References

1 R. Sh. Mikhail, D. Dollimore, A. M. Kamel and N. R. El-Nazer, J. Appl. Chem. Biotech., 23 (1973) 419.

2 R. Sh. Nikhail, D. Dollimore, A. M. Kamel and N. R. El-Nazer, J. Appl. Chem. Biotech., 23 (1973) 431.

3 F. A. Kroger and J. H. Vink, Solid State Physics, vol. 3 (F. Seitz and D. Turnbull, Eds) Academic Press, New York 1956, p. 307.

4 D. Dollimore and J. Pearce, J. Thermal Anal., 6 (1974) 321.
5 D. Dollimore, J. A. France, B. W. Krupay and R. Whitehead, Thermochim. Acta, 36 (1980) 343.
6. D. Dollimore and P. R. Rodgers, Thermochim. Acta, 30 (1979) 273.
7 D. Dollimore, G. R. Heal and R. W. Krupay, Thermochim. Acta, 24 (1978) 293.
8 D, Dollimore and T. J. Taylor, Thermochim. Acta, 40 (1980) 279.
9 D. A. Young, The International Encyclopedia of Physical Chemistry and Chemical Physics, Vol. 21, Decomposition of Solids, Pergamon Press, Oxford 1966.
10 M. E. Brown, D. Dollimore and A. K. Galwey, Comprehensive Chemical Kinetics, Vol. 22, Reactions in the Solid State, (C. H. Bamford and C.F. Tipper, Eds) Elsevier, Amsterdam 1980.
11 N. A. Carthey, D. H. Kerridge and S. A. Tariq, Thermochim. Acta, 61 (1983) 185.
12 C. Duval, Inorganic Therm. Anal., Elsevier, Amsterdam 1964.
13 W. R. Pease, R. L. Segal, R. L. Smart and P. S. Turner, J. Chem. Soc. Faraday Trans. 1, 83, (1986) 747.
14 CRC Handbook of Chemistry and Physics, 2nd Ed., 1981.
15 J. H. Sharp, G. W. Brindley and B. N. Achar, J. Amer. Ceram. Soc., 49 (1966) 379.
16 L. Reich, H. T. Lee and D. W. Levi, J. Polym. Sci., Part B, 1 (1963) 535.
17 H. E. Kissinger, J. Res. Nat. Bur. Stand., 57 (1956) 217; Anal. Chem., 29 (1957) 1702.
18 G. M. Schwab and G. M. J. Schmidt, J. Appl. Phys., 33 (1962) 426.
19 P. W. M. Jacobs and A. R. Tariq Kureisky, Trans Faraday Soc., 58 (1962) 552; Proc. Fourth International Symposium on the Reactivity of Solids, Elsevier, Amsterdam 1960, p. 361.
20 A. K. Galwey, Adv. Catal., 26 (1977) 247.
21 E. Cremer, Adv. Catal., 7 (1955) 75.
22 G. C. Bond, Catalysis by Metals, Academic Press, New York 1962.
23 J. Sestak, Thermophysical Properties of Solids, Vol. XII Part D. of Comprehensive Analytical Chem. (Ed. G. Svehla) Elsevier, Amsterdam 1984, 202.
24 E. Koch, Non-Isothermal Reaction Analysis, Academic Press, London 1977.

Zusammenfassung — Thermische Analysemethoden wurden zur Ermittlung der Zersetzungsart von Nickelkarbonaten eingesetzt, die auf dem Wege der Kopräzipitation versetzt wurden. Das auf diese Weise präparierte Nickelkarbonat hat die Stöchiometrie $x\mathrm{NiCO_3}.y\mathrm{Ni(OH)_2}z\mathrm{H_2O}$. Die Bestimmung des Zersetzungsmechanismus erfolgte mittels isothermer Thermogravimetrie. TG und DSC wurden zur Untersuchung der Auswirkung der Versetzung auf die Zersetzungskinetik eingesetzt. Man fand, daß die Zersetzung stark von der Versetzung beeinflußt wird. Die Kinetik der thermischen Zersetzung der versetzten Karbonate wurde mit Leitfähigkeitsstudien verglichen. Bei der thermischen Zersetzung von versetzten Nickelkarbonaten wurde ein Kompensationseffekt beobachtet und diskutiert.